Complex Formation of Chitosan with Iodine and its Structure and Spectroscopic Properties – Molecular Assembly and Thermal Hysteresis Behavior[1]

Hirofumi Yajima,[2,6] Masataka Morita,[3] Masanori Hashimoto,[4] Takeshi Kikuchi,[5] and Tadahiro Ishii[2]

[1] Paper presented at the Fourteenth Symposium on Thermophysical Properties, June 25-30, 2000, Boulder, Colorado, U.S.A.

[2] Department of Applied Chemistry, Faculty of Science, Science University of Tokyo, 1-3 Kagurazaka, Shinjuku-ku, Tokyo 162-8601, Japan

[3] Design Department, Science Instruments Division, Hitachi Koki Co., Ltd., 1-24-12, Nishi-Shinbashi Minato-ku, Tokyo 105-8717, JAPN

[4] Project Execution Department, Environmental Consulting and Engineering Division, Kurita Water Industries Ltd., 4-7, Nishi-Shinjuku 3-Chome, Shinjuku-Ku, Tokyo 160-8383, Japan

[5] Department of Chemical Technology, College of Science and Industrial Technology, Kurashiki University of Science and the Arts, 2640 Nishinoura, Tsurajima-cho, Kurashiki, Okayama 712-8505, Japan

[6] To whom correspondence should be addressed.

ABSTRACT

To elucidate the factors responsible for the complexation of chitosan with iodine and to gain insight into the structures and spectroscopic properties of chitosan-iodine (CI) complexes, extensive studies were performed of the effects of iodine/chitosan concentrations and temperature on CI complexation and its physicochemical properties in acetic buffer solutions containing excess KI by means of various spectroscopic (absorption, CD etc.) and structural-analysis (SAXS etc.) measurements and MD simulations. CI complex exhibited absorption spectra with a peak at around 500 nm, regardless of the iodine/chitosan concentrations and temperature. Correspondingly, the CI complexes exhibited mutually split CD bands with opposite signs (+, -) at around 500 nm. The CI complex showed thermal hysteresis, i.e., an irreversible reaction process involved in complexation and color formation. Resonance Raman spectra measurements revealed that the iodine species responsible for the purple coloring of the complexes is primarily I_3^- ions. Moreover, ^{13}C-NMR spectra measurements inferred that the interaction sites in the D-glucosamine moiety in chitosan chains with bound iodine are hydroxyl groups on C-1, C-3 and C-4. Structural studies based on analytical ultracentrifugation, SAXS and SANS measurements indicated that the molecular assembly of extended chitosan chains plays an important role in CI complexation. MD calculation predicted that the irreversibility and thermal hysteresis behavior of the CI complexes are due to a crystalline-like extended $\rightarrow$ compact folded conformational transition.

KEY WORDS: chitosan-iodine complex; molecular assembly; molecular simulation; physicochemical properties; structural analysis; thermal hysteresis behavior.

1. INTRODUCTION

Chitosan, a linear polysaccharide of β-(1,4) linked D-glucosamine, obtained primarily as a by-product of the seafood industry, has recently attracted a great deal of attention as a multifunctional biopolymer for industrial, agricultural, medical and pharmaceutical applications because of its unique properties including a variety of biological activities, biodegradability, biocompatibility, its behavior as a polyelectrolyte, metal-chelating function, flocculation etc. [1-4]. Chitosan is an acid-soluble and N-deacetylated derivative of chitin, which is widely distributed in nature in bacterial cell walls and in the exoskeletons of crustaceans and insects [1]. For improvement and further development of the potential applications of chitosan, it is necessary to gain great information of its molecular characteristics based on extensive physicochemical studies.

The chain conformations of chitosan molecules in the solid state in the free anhydrous chitosans, acid salts and transition metal complexes have been studied by various structural analysis techniques such as X-ray diffraction [5-8] and solid-state ^{13}C NMR [9]. Chitosan chains have been reported to adopt an extended 2-fold helical conformation stabilized by the O3---O5 hydrogen bond or an extended left-handed 8/5 helical conformation. In addition, X-ray diffraction studies of the molecular and crystal structure of hydrated chitosan by Okuyama et al. [10] revealed that chitosan in the hydrated form adopts a 2-fold helix chain conformation similar to that in the anhydrate, and water molecules contribute to stabilization of the structure by forming water-bridges between polymer chains. On the other hand, a number of studies on the solution properties of chitosan molecules have been also performed by means of various techniques such as viscosity measurement [11-14], static and dynamic light scattering [11,14,15], NMR [16], and the Monte Carlo calculation [17]. The characteristics of

chitosan are dependent on the degree of deacetylation (DDA), the distribution of acetyl groups, chain length and molecular weight distribution. Chitosans with different DDs under different solution conditions (different ionic strength, pH, or temperature) are predicted to be in rod shaped or a stiff coil [12-14,17], a random coil [12-14,18] , or a compacted sphere [19] depending on the variables.

Chitosan has been shown to form a colored complex with iodine as seen in the blue iodine complexes of amylose [20-22] and poly(vinyl alcohol) [23,24]. This reaction has been used for the chitosan test [25-27]. Shigeno et al. [28,29] studied the adsorption behavior of iodine on chitosan films by physicochemical methods. They reported that iodine adsorption was caused by the formation of charge-transfer complexes between the amino groups of chitosan and iodine molecules. Recent X-ray structural analysis of the CI complex by Okuyama et al. [30] revealed that the chitosan chain in the CI crystal adopts a new type 4/1 helical conformation alternative to the 2/1 or 8/5 helical types. With reference to the biological activities of the chitosan-iodine (CI) complex, Sashiwa et al. [31] showed that partially deacetylated chitin-Isodine suspension has antimicrobial and wound healing activities.

From the objective of more effective utilities of chitosan and iodine as natural resources and the development of their novel functions, we have investigated the physicochemical properties, in particular, the coloring mechanism and structure of the CI complexes in solution [32,33], in comparison with the amylose-iodine (AI) complexes. Our results can be summarized as follows: (A) When chitosan powder was directly dissolved in KI-I_2 solution containing acid (HNO_3, acetate buffer etc.) at room temperature, the complexation was recognized by specific coloring. (B) However, when chitosan solution containing acid was mixed with KI-I_2 solution at room temperature, complexation did not occur. (C) The color of the complex solution in (A) vanished

when the temperature was raised to ca.80°C, but recovery of the color was not observed even if the temperature was then lowered to 4°C. (D) When the uncomplexed (B) and (C) solutions were frozen, they developed the same color as the (A) solution. These observations indicated that thermal hysteresis, i.e., an irreversible reaction process, is involved in complexation and color formation. There is as yet no clear concerns regarding the relationship between the thermal hysteresis phenomenon and the molecular characteristics, in particular solution structure of the CI complexes.

The present study was performed to analyze the spectroscopic properties of the CI complexes and to characterize the solution structures of chitosan and the CI complexes by various physicochemical techniques including circular dichroism (CD), resonance Raman spectroscopy, small-angle X-ray/neutron scattering (SAXS/SANS) measurements and molecular dynamics (MD) calculations. We will also discuss the factors responsible for CI complexation and the thermal hysteresis behavior.

2. EXPERIMETAL

2.1. Materials

Chitosan (C-9) from queen crab shell was supplied by Kurita Water Industries Ltd. and used without further purification. Its weight-average molecular weight (M_w) and molecular weight distribution (M_w/M_n) were M_w = 1.1 x 10^4 and M_w/M_n = 2.2, respectively, as determined by size-exclusion chromatography coupled to a multiple-angle laser light-scattering (SEC-MALLS) using DAWN-E model system (Wyatt Tech.). The DDA value of chitosan was 98% as determined by colloidal titration [34].

2.2. Preparation of CI complexes

The CI complexes were prepared by freezing mixtures of chitosan and KI-I_2 solutions and thawing them at 4°C. CI complex solutions were prepared over a wide

concentration range of chitosan from 5 x 10^{-3} - 0.2 uM (u refers to one β-D-glucosamine unit) and I_2 5 x 10^{-4} - 3.5 x 10^{-3} M under the conditions of [KI]/[I_2] = 10. The main solvent used in this study was aqueous acetate buffer (0.3 M AcOH + 0.1 M NaOAc, pH 4.0). For SANS measurements with the contrast variation method [35], deuterated acetate buffer in heavy water D_2O was used, and the CI complex solutions were prepared using the mixed solvents of D_2O/(the D-buffer) and H_2O/(the H-buffer) with different D_2O contents (ϕ_D). As the other acidic solvent for resonance Raman and ^{13}C-NMR measurements, 0.13 M HNO_3 aq was used.

For preparation of thermally treated CI complex solutions, the samples were heated in sealed tubes to a given temperature and allowed to stand at this temperature for 10 min, then cooled to room temperature. This method was based on irreversibility of the CI complexation and the treated samples were confirmed to be of the same color as those in situ at a given temperature.

2.3. Measurements

Absorption and CD spectra of the complexed solutions were obtained using a Shimazu UV-2101PC spectrophotometer and Jasco J-725 spectropolarimeter, respectively. The light path length of the cell was 1mm for both absorption and CD measurements. Raman spectra were measured with a Jasco NR-1000 spectrophotometer using an Ar^+ ion (514.5 and 488.0 nm) laser for excitation with a rotary cell. ^{13}C-NMR measurements were performed on a JEOL JNM-EX400 NMR spectrometer.

Apparent sedimentation coefficients ($S^{app}_{20,W}$) and molecular weights (M^{app}) of the CI complexes were determined at 20°C by the sedimentation velocity method and sedimentation equilibrium method [36] using a Hitachi CP100α ultracentrifuge with an attached ABS-8 analytical UV monitor with the Hitachi software program. M^{app} were

estimated from the Lamm equation:

$$M_{app} = \frac{2RT}{(1-V\rho)\omega^2} \mathrm{x} \frac{d \ln A}{dr^2} \qquad (1)$$

where A = absorbance at a given wavelength, which is proportional to the CI concentration and is measured with absorption optics; r = distance from center of rotation; V = partial specific volume of the solute; ρ = density of solvent; ω = angular velocity of rotor; R = gas constant; T = absolute temperature. In this study, V was taken to be 0.6 for all samples, referring to the average value of general polysaccharides [37].

SAXS measurements were performed at 25°C in the range of the scattering vector q (= $4\pi\sin(\theta/2)/\lambda$) of 6 x 10^{-3} - 0.2 $Å^{-1}$ using a SAXS spectrometer installed at the BL-10C port in the Photon Factory of the National Laboratory for High Energy Accelerator Research Organization (Tsukuba, Japan). Sample-to-detector distance and wavelength λ were 188 cm and 1.49 Å, respectively. Structural analysis from the total scattering curve was carried out by calculating the distance distribution function, $p(r)$, given by Fourier inversion of the scattering intensity $I(q)$ as

$$p(r) = \frac{2}{\pi}\int_0^\infty rqI(q)\sin(rq)\, dq \qquad (2)$$

Then, the radius of gyration, Rg, was estimated by the equation [38]:

$$Rg^2 = \frac{\int_0^{D_{max}} p(r)r^2 dr}{2\int_0^{D_{max}} p(r) dr} \qquad (3)$$

where D_{max} is the maximum dimension of the particle estimated from the condition p(r) = 0 for r > D_{max}.

SANS measurements with the contrast variation method [24,35] were carried out at 20°C using a SANS spectrometer (SANS-U) installed at the C1-2 port of the cold-neutron beam line in the research reactor JRR-3M of the Japan Atomic Energy Research

Institute (JAERI), Tokai, Japan. The wavelength used was 7.0 Å and the sample-to-detector distance was 4m (8×10^{-3} Å^{-1} < q < 7×10^{-2} Å^{-1}) and 1m (4×10^{-2} Å^{-1} < q < 0.25Å^{-1}). Structural analyses were performed based on the Stuhrmann plot from the SANS data. This procedure was described in detail elsewhere [24,35].

2.4. MD Calculations

Prediction of the changes in the solution conformation of chitosan in the annealing process was carried out by the 500 ps MD calculation using the Discover module (CVFF as force field) of INSIGHT II from Molecular Simulation, Inc. under the conditions of distance-dependent dielectric constants (ε = 1.8r) with no cut-off for all interactions according to the following procedures [33,39]: (1) The relaxed potential energy map of chitobiose (chitosan dimer) was determined based on the CVFF force field by optimizing the structures on a 10° grid spacing of the torsional angles about the glycosidic bonds (ϕ,φ), referring *the Cambridge Structural Database* (CSD) for an initial structure. (2) The molecular models as starting samples for the MD calculation were constructed for chitosans with degrees of polymerization (DP) of 20, 30 and 50 based on the dimer structure of the energy minimum. (3) MD calculations for the heating process were carried out at 298 K and then at 1200 K, where a number of conformations were generated. (4) MD calculations in the cooling process from 1200 K were made stepwise at 500 K and then at 298 K for each of several 1200K-generated conformations selected randomly as starting samples. The conformations at 298 K were confirmed to become stable with small energy fluctuation around equilibrium state at the final stage in the 500 ps calculation. (5) For comparison, the same MD calculation was carried out for amylose chains.

3. RESULTS AND DISCUSSION

3.1. Spectroscopic properties

Figures 1 (a) and (b) show typical absorption and CD spectra of the purple-colored CI complex, including the I_2 concentration dependences of the absorbance (A_{500}) and ellipticities (θ_{460}, θ_{540}) at the maximum wavelengths at a given concentration of chitosan. As a reference the absorption spectrum for free I_2/KI solution is also shown. The complex exhibited an absorption spectrum with a peak at 500 nm, and mutually split CD bands with opposite signs (+,-). It should be noted that these spectral characteristics were independent of the concentrations of iodine and chitosan, temperature and acid species [32], and were similar to those of AI complexes [20]. We have concluded that the coloring of AI complexes was developed by the left-handed *iodine/iodide dimer exciton-coupled mechanism* involving *charge-transfer* between iodine/iodide and amylose chain and the *configuration interaction* among the electronic transition states of iodine/iodide [20,22]. The coloration of the CI complexes could be interpreted in terms of a similar mechanism.

A sharp increase in the A_{500} value with I_2 concentration appeared at a threshold I_2 concentration ($[I_2]/[\text{chitosan}] \approx 0.05$) in accordance with the increase in θ_{460} and θ_{540}, up to a high concentration (3.5×10^{-3} M), above which precipitation of the CI complexes was observed. The A_{500} values tended to increase with chitosan concentration in accordance with the increase in θ_{460} and θ_{540} drawing a sigmoidal curve up to a high concentration, but then decreased above this concentration [40]. The extent of the coloring decay in the high concentration range of chitosan was enhanced with aging time after complex preparation. This was taken to be due to hydrolysis of I_2 through the reaction of basic glucosamine resides and water.

The effects of temperature on the optical quantities in the heating and cooling processes are shown for A_{500} and θ_{460} or θ_{540}, respectively, in Fig.2(a) and (b), where

heating and cooling rates were adjusted to 2°C/min with a thermostated cell controller. In the heating process, both of the optical quantities decreased sharply above 30°C and then the color completely disappeared at ca. 60°C. On the other hand, in the cooling process after the disappearance of the color, the neither of the optical quantities recovered even if the temperature was lowered to 4°C. However, when the solution was frozen and then thawed, the optical quantities showed complete recovery. These results indicated that CI complexation is essentially irreversible, in contrast to AI complexation [41]. We confirmed that the recovery for this thermal hysteresis behavior could be repeated at least 5 times. It should be noted that we have not yet determined the mechanism of coloring recovery induced by freezing of the chitosan mixed solution.

The resonance Raman spectra of the CI complex in HNO_3 aq are shown in Fig.3 with respect to the 488.0- and 514.5-nm excitation. The Raman spectrum of free I_2-KI solution is included as a reference. Raman spectra exhibited strong scattering at 110 cm^{-1} and weaker scattering at 150 cm^{-1} as fundamental tones regardless of the excitation wavelength. In addition, an overtone band at 110 cm^{-1} appeared at 220 cm^{-1}. Similar spectral characteristics were obtained in the other acid-species systems. The other iodine/iodide complexes of amylose [42] and poly(vinyl alcohol) [43] also had similar fundamental Raman lines (160 and 110 cm^{-1}), although the 160-cm^{-1} lines in their Raman spectra were stronger than the 110-cm^{-1} lines. The 110-cm^{-1} lines of the CI complex and free iodine/iodide were assigned to the I_3^- symmetric stretching vibration, whereas the 150-cm^{-1} line was assigned to the I_5^- asymmetric stretching vibration [42-44]. Therefore, it was concluded that the bound iodine species responsible for the coloring of CI complexes is primarily I_3^- ions.

To obtain information regarding the iodine-binding sites of glucosamine residues, the changes in the chemical shifts in the ^{13}C-NMR spectra of chitosan induced by CI

complexation were examined. The ^{13}C-NMR spectrum of the CI complex in HNO_3 aq measured using MeOH as an external reference is shown in Fig.4, where the assignment of each of the signal peaks is given in the figure [16]. The effect of the iodine-binding on the chemical shift of each peak is summarized in Table 1. Only C-1, C-3, and C-4 signals are shifted to a higher field due to the effect of heavy atoms such as iodine on the nuclear shielding constant [45]. Similar results were obtained in the other acid-species systems in the same way as for the other spectral characteristics. Therefore, the interaction sites in the glucosamine residues in chitosan with bound iodine were inferred to be OH groups or glycosidic oxygen atoms on C-1, C-3 and C-4, and the amino group for C-2 was not responsible for the binding of iodine.

3.2. Structural Studies

Apparent molecular weights (M^{app}) of the CI complexes, estimated from Eq.(1) by sedimentation equilibrium measurements under conditions of $[I_2]/[\text{chitosan}] = 0.1$, are summarized as a function of treatment temperature in Fig.5. It should be noted that the treated samples were confirmed to hold the same coloring abilities as those in situ at each temperature from the irreversibility of the complexation, as described in "**EXPERIMENTAL 2.2.**". Surprisingly, the M^{app} value at 20°C was 3.8×10^5 ($S_{20,W}$ = 13.0 S), about 35-fold higher than that of intact chitosan ($M^{app} = 1.1 \times 10^4$, $S_{20,W}$ = 0.4 S), which coincided with the M_w value determined from the SEC-MALLS measurement. The M^{app} value decreased markedly above 30°C with temperature, conforming to the coloring decline, and approached the M^{app} value of intact chitosan. In view of the observation that the relative number of glucosamine residues to one I_2 molecule was 10 in this experiment, this result implies that the molecular assembly of chitosan through the interaction with iodine plays an important role in colored CI complexation associated with the effect of iodine and/or chitosan concentrations on

complexation.

Subsequently, the characterization of aggregate structures of the CI complexes was carried out based on analyses of the SAXS data. Figure 6 shows the observed SAXS curves of chitosan and the CI complex at 25°C, where the signal-to-noise ratio for chitosan is small owing to the low $I(q)$, including the distance distribution functions, $p(r)$ (Eq.(2)). The Rg values estimated from the $p(r)$ functions were 27.3 Å (D_{max} = 55 Å) for chitosan and 78.2 Å (D_{max} = 190 Å) for the CI complex, which corresponded to a significant increase in the M^{app} value following the complexation. From the viewpoint of the resulting p(r) shapes, simulation of the $p(r)$ curves of chitosan and the CI complex was carried out with the theoretical scattering functions for an ellipsoid and a cylinder composed of two layers [46], respectively. As a result of fitting to the Rg values as well as the $p(r)$ curves, the solution structure of chitosan was characterized by the ellipsoid with a major semiaxis of 30 Å and minor semiaxis of 10 Å, whereas the aggregate structure of the CI complex was characterized by a cylinder with a height of 210 Å, inner radius of 10 Å, and outer radius of 20 Å, assuming that the inner scattering density was about two-fold larger than the outer density. The resulting $I(q)$ and $p(r)$ functions corresponding to each of the theoretical models are shown in solid lines in Fig.6. Taking account of the virtual bond length of 5.5 Å between the glucosamine residues and the average DP (ca. 70) of chitosan used in this study, it is conceived that free chitosan takes a compactly folded conformation involving intramolecular hydrogen bonds, whereas the chitosan chains in the CI aggregate take a crystalline-like extended conformation [5-8,10,31]. The two-layer cylindrical model for the aggregate structure of the CI complex was supported by the results of structural analysis of the SANS data based on the Stuhrmann plot [35,46], in which the Rg value at infinite contrast (Rg,c), the radial second moment of the mean scattering length density (SD), α, and the

derivation of the center of the SD distribution, β, were estimated to be Rg,c = 91.6 Å, α = -74.2 and β = 0 Å^{-2}, respectively. For intact chitosan, these values were Rg,c = 40.4 Å, α = -10.0, and β = 29.6 x 10^{-10} Å^{-2}. Further details of the SANS studies will be reported elsewhere. SAXS and SANS structural analyses suggested that the CI complex forms an aggregate with a two-layer cylindrical structure composed of an inner polyiodide chain surrounded by an assembly of crystalline-like extended chitosan chains involving intermolecular hydrogen bonds network. This structural characteristic of the CI complex would be analogous to that proposed for poly(vinyl alcohol)-iodine complex [23,24], but differ from that of the AI complex in which iodine/iodide molecules are included in sixfold, left-handed helical V-amylose [47]. One of our findings, (A) described in the "**INTRODUCTION**", could be interpreted in terms of the requirement of the crystalline-like extended chitosan chains for coloring of the complex.

Figure 7 shows the effects of treatment temperature on the Rg values estimated by Eq.(3) from the $p(r)$ functions. The Rg value tended to decrease with the temperature above 30°C, corresponding to the M^{app} behavior (see Fig.5), followed by a decline in color. The above results including the $p(r)$ functions suggested that the aggregate structure the CI complex starts to be destroyed at ca. 30°C , followed by dissociation of the intermolecular hydrogen bond networks of chitosan chains and the release of bound iodine/iodide, and that the complex is transformed with temperature from a cylindrical structure to a compacted ellipsoid or spherical structures of free chitosan chains.

3.3. MD Calculations

To determine the factors involved in the irreversibility of CI complexation, the solution conformations of chitosan chains were predicted according to the procedures described in "**EXPERIMENTAL 2.4.**", in comparison with that for amylose chains. The current lowest energy conformation of a long chitosan chain was predicted to be an

extended conformation similar to the crystalline conformation [10] based on the torsion angles ($\phi = 45.7°$, $\varphi = -14.4°$) for the energy minimum in the counter map of chitobiose, whereas the current lowest energy conformation of the amylose chain was predicted to be a similar 6/1 helical structure to the crystalline conformation [47] from the torsion angles ($\phi = -11.6°$, $\varphi = -18.2°$) for the maltose energy minimum. MD simulations for the chitosan and amylose chains in the heating (298 $\rightarrow$ 1200K) and cooling (1200 $\rightarrow$ 298 K) processes were carried out using the predicted extended and 6/1 helical structures, respectively, as starting samples. The MD simulations showed that the extended conformation of chitosan tends to be transformed to a folded conformation like an antiparallel β-sheet of protein, and the folded conformation could not be returned easily to the extended form by decreasing temperature. In contrast, the final conformation of the amylose chain fluctuated around an original helical structure and could be recovered by cooling. The β-sheet-like folded conformations of chitosan are located close to the lowest energy extended conformation, but the distribution of states is highly rugged and this would result in a long half-life of trapped states at one of the folded conformations, as suggested by the random energy model [48]. These conformational properties of chitosan are likely to be responsible for the irreversibility of CI complexation. It should be noted that the theoretical scattering function and the *p*(r) function for the compactly folded conformations were in good agreement with the experimental results. Further details of the MD simulation will be reported elsewhere.

In summary, the results of the present study indicated that a stable conformation of chitosan in solution would be a folded structure, that does not form a colored complex with iodine, and the irreversibility and thermal hysteresis behavior as a unique characteristic of CI complexes would be governed by a crystalline-like extended $\rightarrow$ compactly folded conformational transition of chitosan in solution.

ACKNOWLEDGMENTS

This work was supported in part by Grand-in-Aid for Scientific Research No. 12650889 from the Minister of Education, Science and Culture of Japan. We are greatly indebted to Mr. Katsunori Tsunoda, Mr. Yoshihiro Suzuki, and Mr. Tetsuya Sakajiri for their technical assistances.

REFERENCES

1. P. A. Sandford, in *Chitin/Chitosan: Sources, Chemistry, Biochemistry, Physical Properties, and Applications*, G. Skjak-Braek, T. Anthonsen, and P. A. Sandford, eds. (Elsevier, Amsterdam, 1990), p.51.
2. P. A. Sandford and G. P. Hutchings, in *Industrial Polysaccharides*, M. Yalpani, ed. (Elsevier, Amsterdam, 1987), p.363.
3. W. Malette, M. Quigley, and E. Adicks, in *Chitin in Nature and Technology*, R. Muzzarelli, C. Jeuniaux, and G. Gooday, eds. (Plenum Press, New York, 1986), p.435.
4. S. Minami, Y. Okamoto, A. Matsuhashi, H. Sashiwa, H. Saimoto, Y. Shigemasa, T. Tanigawa, Y. Tanaka, and S. Tokura, in *Advances in Chitin and Chitosan*, C. J. Brine, P. A. Sandford, and J. P. Zikakis, eds. (Elsevier Applied Science, London, 1992), p.61.
5. K. Ogawa and S. Inukai, *Carbohydr. Res*., **160**: 425 (1987).
6. T. Yui, K. Imada, K. Okuyama, Y. Obata, K. Suzuki, and K. Ogawa, *Macromolecules*, **27**: 7601 (1994).
7. K. Mazeau, W. T. Winter, and H. Chanzy, *Macromolecules*, **27**: 7606 (1994).
8. A. Yamamoto, J. Kawada, T. Yui, and K. Ogawa, *Biosci. Biotech. Biochem*., **61**: 1230 (1997).
9. H. Saito, R. Tabeta, and K. Ogawa, *Macromolecules*, **20**: 2424 (1987).
10. K. Okuyama, K. Noguchi, T. Miyazawa, T. Yui, and K. Ogawa, *Macromolecules*, **30**: 5849 (1997).
11. M. Terbojevich, A. Cosani, B. Focher, A. Naggi, and G. Torri, *Carbohydr. Polym*., **18**: 35 (1992).
12. M. W. Anthonsen, K. M. Vårum, and O. Smidsrød, *Carbohydr. Polym*., **22**: 193

(1993).

13. N. Errington, S. E. Harding, K. M. Vårum, and L. Illum, *Int. J. Bio. Macromol*., **15**: 113 (1993).
14. M. L. Tsaih and R. H. Chen, *Int. J. Bio. Macromol*., **20**: 233 (1997).
15. R. G. Beri, J. Walker, E. T. Reese, and J. E. Rollings, *Carbohydr. Res*., **238**: 11 (1993).
16. A. Domard, C. Gey, M. Rinaudo, and C. Terrassin, *Int. J. Biol. Macromol*., **9**: 233 (1987).
17. T. Yui, H. Kobayashi, S. Kitamura, and K. Imada, *Biopolymers*, **34**: 203 (1994).
18. C. Yomota, T. Miyazaki, and S. Okada, *Colloid. Polym. Sci.*, **271**: 76 (1993).
19. L. A. Berkovich, G. I. Timofeyeva, M. P. Tsyurupa, and V. A. Davankov, *Polym. Sci. USSR*, **22**: 2009 (1980).
20. T. Handa and H. Yajima, *Biopolymers*, **18**: 873 (1979).
21. T. Handa and H. Yajima, *Biopolymers*, **20**, 2051 (1981).
22. H. Yajima, T. Nishimura, T. Ishii, and T. Handa, *Carbohydr. Res*., **163**: 11 (1987).
23. H. Takamiya, Y. Tanahashi, T. Matsuyama, T. Taniguchi, K. Yamaura, and S. Matsuzawa, *J. Appl. Polym. Sci*., **50**:1807 (1993).
24. H. Yajima, *J. Cryst. Soc. Jpn.*, **36**: 142 (1994).
25. F. L. Campbell, *Ann. Entomol. Soc. Am.*, **22**: 401 (1929).
26. B. D. E. Gaillard and R. W. Bailey, *Nature*, **212**: 202 (1966).
27. R. A. A. Muzzarelli, in *Chitin* (Pergamon, New York, 1977), p.150.
28. Y. Shigeno, K. Kondo, and K. Takemoto, *J. Appl. Polym. Sci*., **25**: 731 (1980).
29. Y. Shigeno, K. Kondo, and K. Takemoto, *Angew. Makromol. Chem*., **91**: 55 (1980).
30. Y. Hanafusa, K. Osawa, K. Noguchi, K. Okuyama, and K. Ogawa, *Polym. Prepr.*

Jpn., **48**: 3853 (1999).

31. H. Sashiwa, Y. Okamoto, S. Minami, and Y. Shigemasa, *Chitin and Chitosan Res*., **4**: 18 (1998).

32.

33. T. Morita, Y. Tezuka, H. Yajima, and T. Ishii, *Polym. Prepr. Jpn*., **46**: 382 (1997).

34. H. Yajima, Y. Suzuki, M. Kamoshita, K. Tsunoda, T. Ishii, and T. Kikuchi, *Polym. Prepr. Jpn*., **47**: 3520 (1998).

35. H. Terayama, *J. Polym. Sci*., **8**: 243 (1952).

36. H. Yajima, H. Yamamoto, M. Nagaoka, K. Nakazato, T. Ishii, and N. Niimura, *Biochim. Biophys. Acta*, **1381**: 68 (1998).

37. A. Tiselius, in *Methods in Enzymology*, Vol. 4, S. P. Colowick and N. O. Kaplan, eds. (Academic Press, New York, 1957), p.35.

37. M. D. Lechner, E. Nordmeier, and D. G. Steinmeier, in *Polymer Handbook*, J. Brandrup E. H. Immergut, and E. A. Grulke eds. (John Wiley & Sons, Inc., 1999), p.VII/85.

38. O. Glatter, in *Small Angle X-ray Scattering*, O. Glatter and O. Kratky, eds. (Academic Press, 1982), p.119.

39. Y. Suzuki, H. Yajima, K. Tsunoda, T. Ishii, and T. Kikuchi, *Polym. Prepr. Jpn*., **48**: 886 (1998).

40. M. Kamoshita, K. Tsunoda, H. Sashiwa, M. Hashimoto, M. Morita, H. Yajima, T. Ishii, Chem. Soc. Jpn. Nat. Meeting, **76**: 763 (1999).

41. G. L. Hatch, *Anal. Chem*., **54**: 2002 (1982).

42. T. Handa and H. Yajima, *Biopolymers*, **19**: 1723 (1980).

43. Y. Oishi, H. Yamamoto, and K. Miyasaka, *Polym. J*., **19**: 1261 (1987).

44. H. Kim, *Biopolymers*, **21**: 2083 (1982).

45. I. Morishima, K. Endo, and T. Yonezawa, *J. Chem. Phys*., **59**: 3356 (1973).

46. L. A. Feigin and D. I. Svergun, in *Structure Analysis by Small-Angle X-ray and Neutron Scattering* (Plenum Press, 1987), p.59.

47. D. French, in *Starch: Chemistry and Technology*, R. L. Whistler, J. N. Bemiller, and E. F. Paschall, eds. (Academic Press, Inc., 1984), p.183.

48. J. D. Bryngelson, J. N. Onuchic, N. D. Socci, and O. G. Wolynes, *Proteins*, **21**: 167 (1995).

Table I. Effects of CI Complexation on Cemical Shifts of the ^{13}C-NMR Signals of β-D-glucosamine Residues

Carbon	Chitosan	CI complex	Δδ (ppm)
C-2	53.848	53.830	-0.018
C-6	58.036	58.036	0.000
C-3	68.259	68.149	**-0.110**
C-5	72.813	72.813	0.000
C-4	74.404	74.367	**-0.037**
C-1	95.764	95.636	**-0.128**

FIGURE CAPTIONS

Fig. 1. Absorption (a) and CD (b) spectra of the CI complex in 0.3 M acetate buffer, including the absorption spectrum of free I_2-KI solution (dotted line). Conc.: [chitosan] = 2 x 10^{-2} uM; [I_2] = 2 x 10^{-3} M; [KI] = 2 x 10^{-2} M. Inset: (a) Absorption (A_{500}) at 500 nm and (b) ellipticities (θ_{460} , θ_{540}) at 460 and 540 nm as a function of I_2 concentration.

Fig. 2. (a) A_{500} and (b) θ_{460} and θ_{540} as a function of temperature. Heating and cooling rates were 2° C/min.

Fig. 3. Resonance Raman spectra of the CI complex in 0.13 M HNO_3 aq excited at 488.0 nm (A) and 514.5 nm (B). The Raman spectrum of free I_2-KI solution excited at 514.5 nm (C) is included as a reference. Conc.: [chitosan] = 5 x 10^{-2} uM; [I_2] = 1 x 10^{-3} M; [KI] = 1 x 10^{-2} M.

Fig. 4. ^{13}C-NMR spectrum of the CI complex in 0.13 M HNO_3 aq using MeOH as an external standard. Conc.: [chitosan] = 0.184 uM; [I_2] = 5 x 10^{-3} M; [KI] = 5 x 10^{-2} M.

Fig. 5. Apparent molecular weight (M^{app}) of the CI complex as a function of treatment temperature in 0.3 M acetate buffer. The broken line refers to the M^{app} value of chitosan. Conc.: [chitosan] = 2 x 10^{-2} uM; [I_2] = 2 x 10^{-3} M; [KI] = 2 x 10^{-2} M.

Fig. 6. Measured SAXS curves of chitosan (a) and the CI complex (b) in 0.3 M acetate buffer. The inset shows the $p(r)$ functions. Solid lines refer to the theoretical $I(q)$ and $p(r)$ functions (see the text for the details). Conc.: [chitosan] = 2 x 10^{-2} uM; [I_2] = 2 x 10^{-3} M; [KI] = 2 x 10^{-2} M.

Fig. 7. Rg estimated from the $p(r)$ functions as a function of treatment temperature. The broken line refers to the Rg value of chitosan.

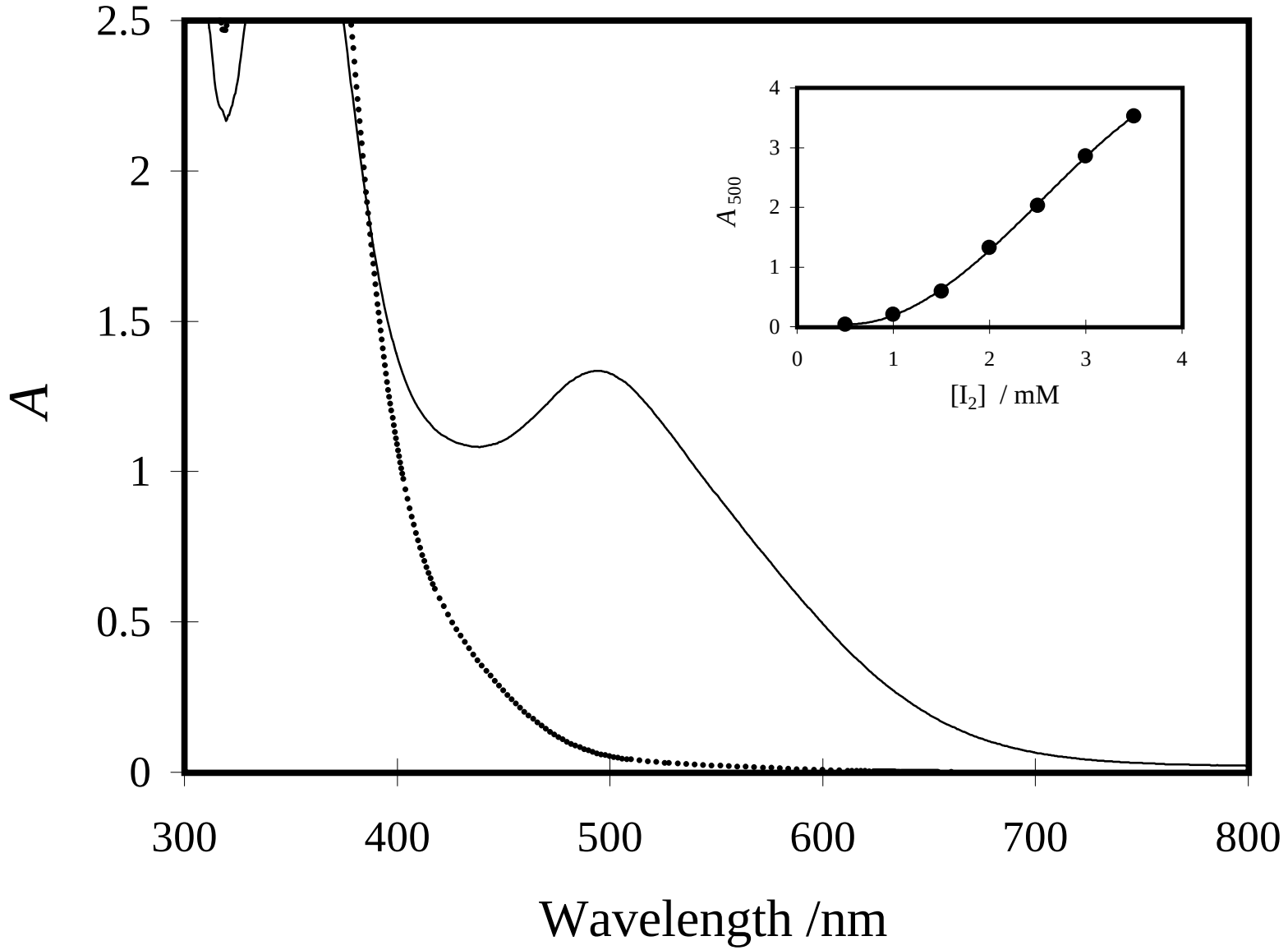

Fig.1(a) H. Yajima

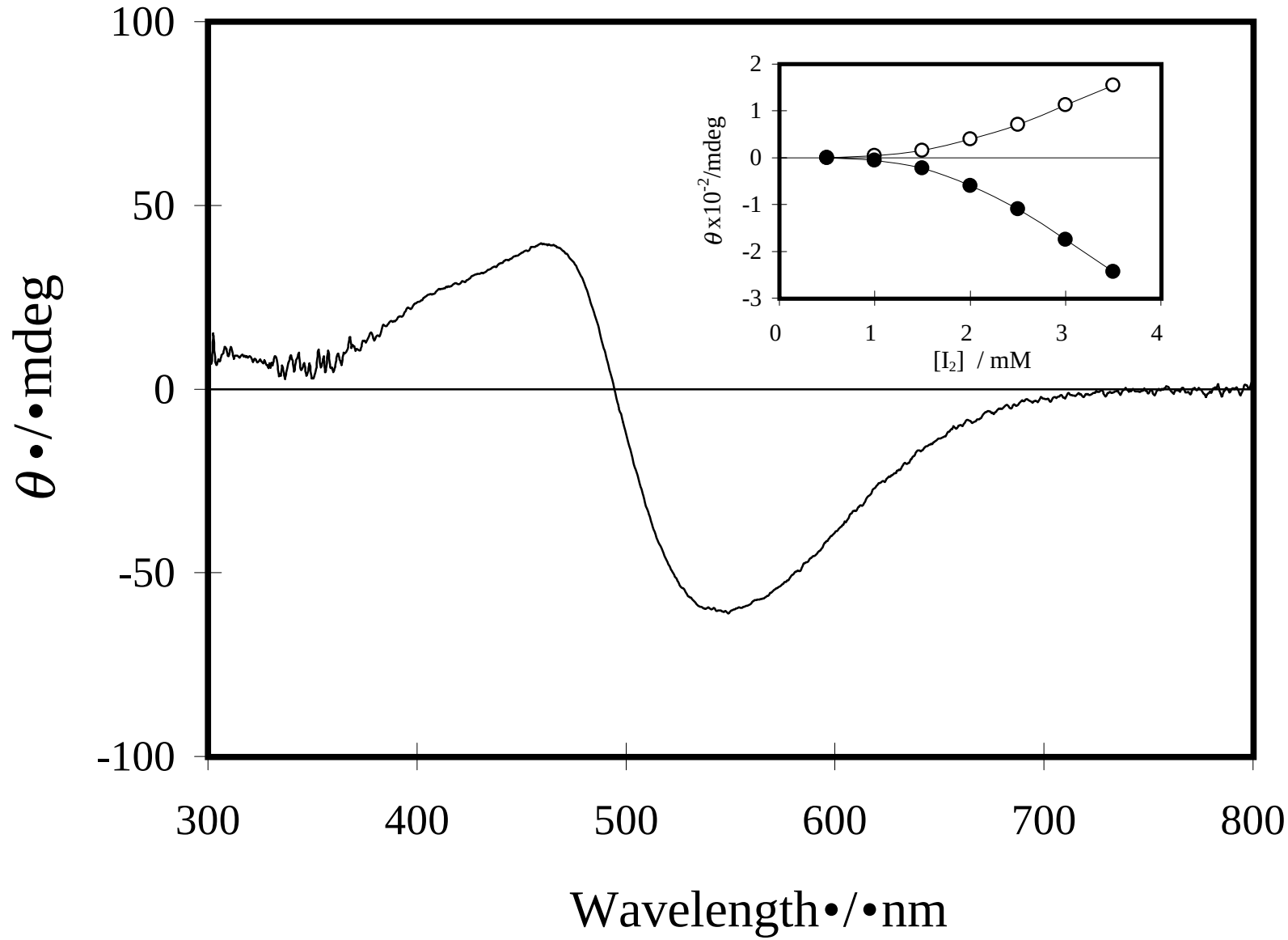

Fig.1(b) H. Yajima

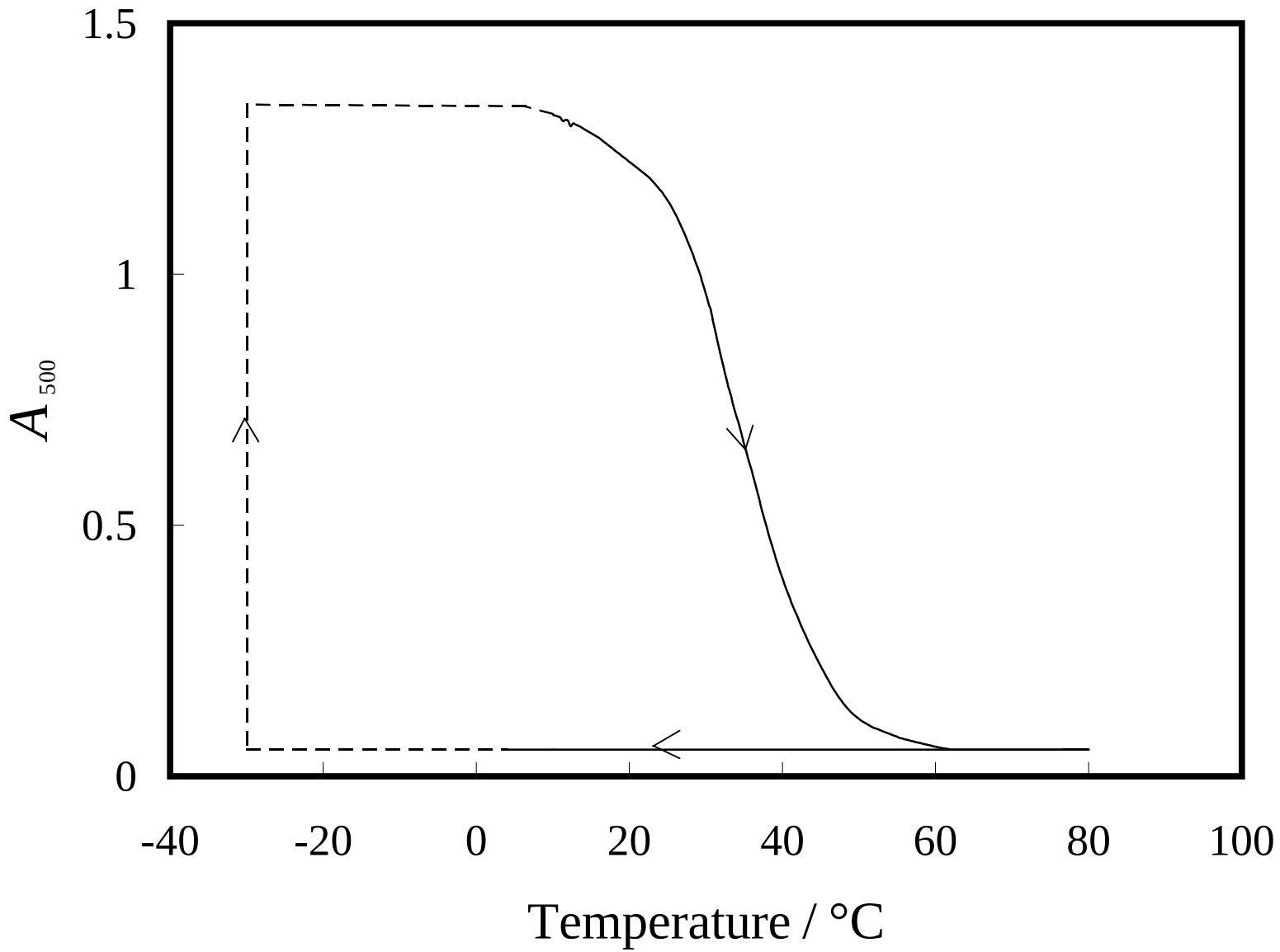

Fig.2(a) H. Yajima

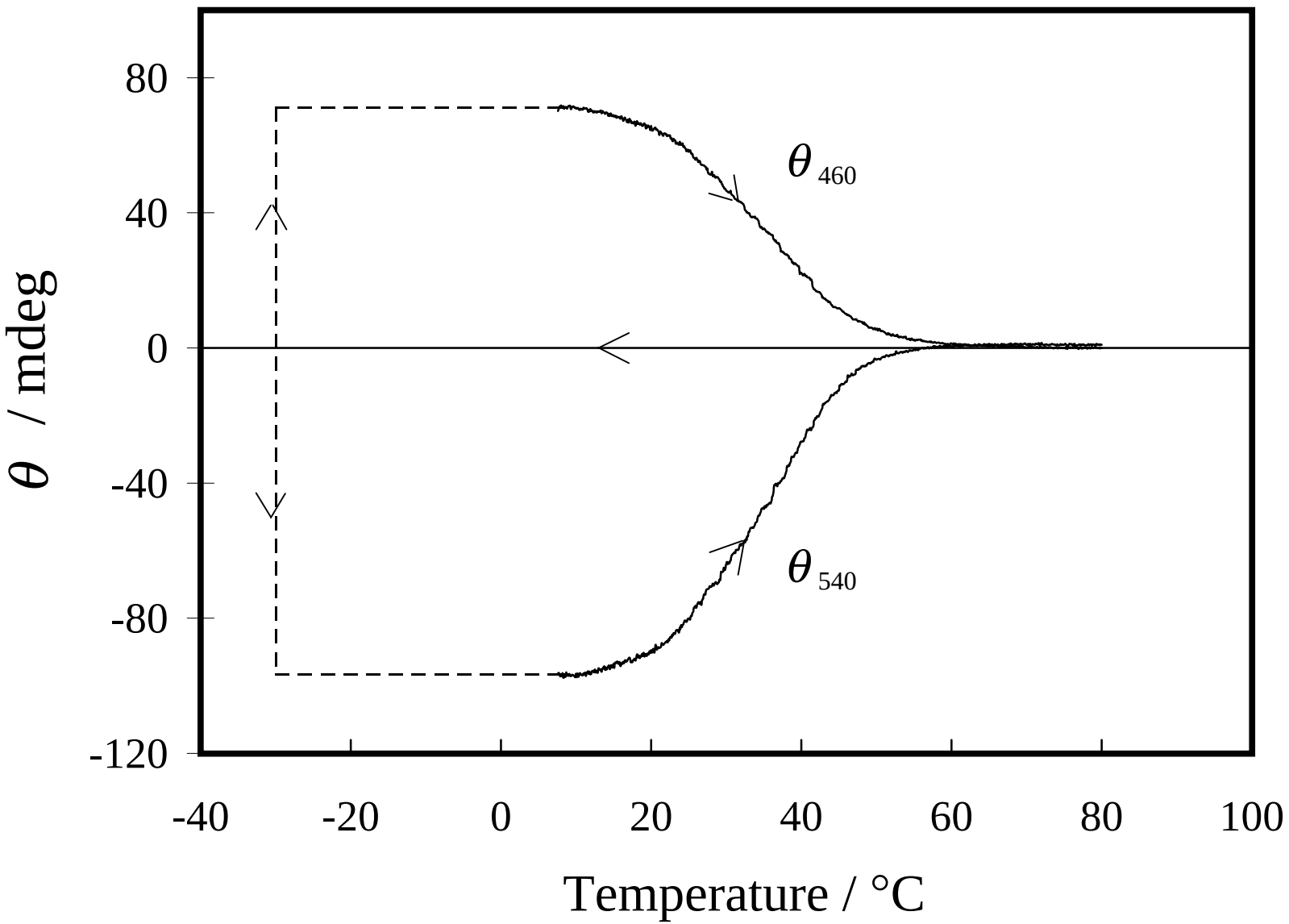

Fig.2(b) H.Yajima

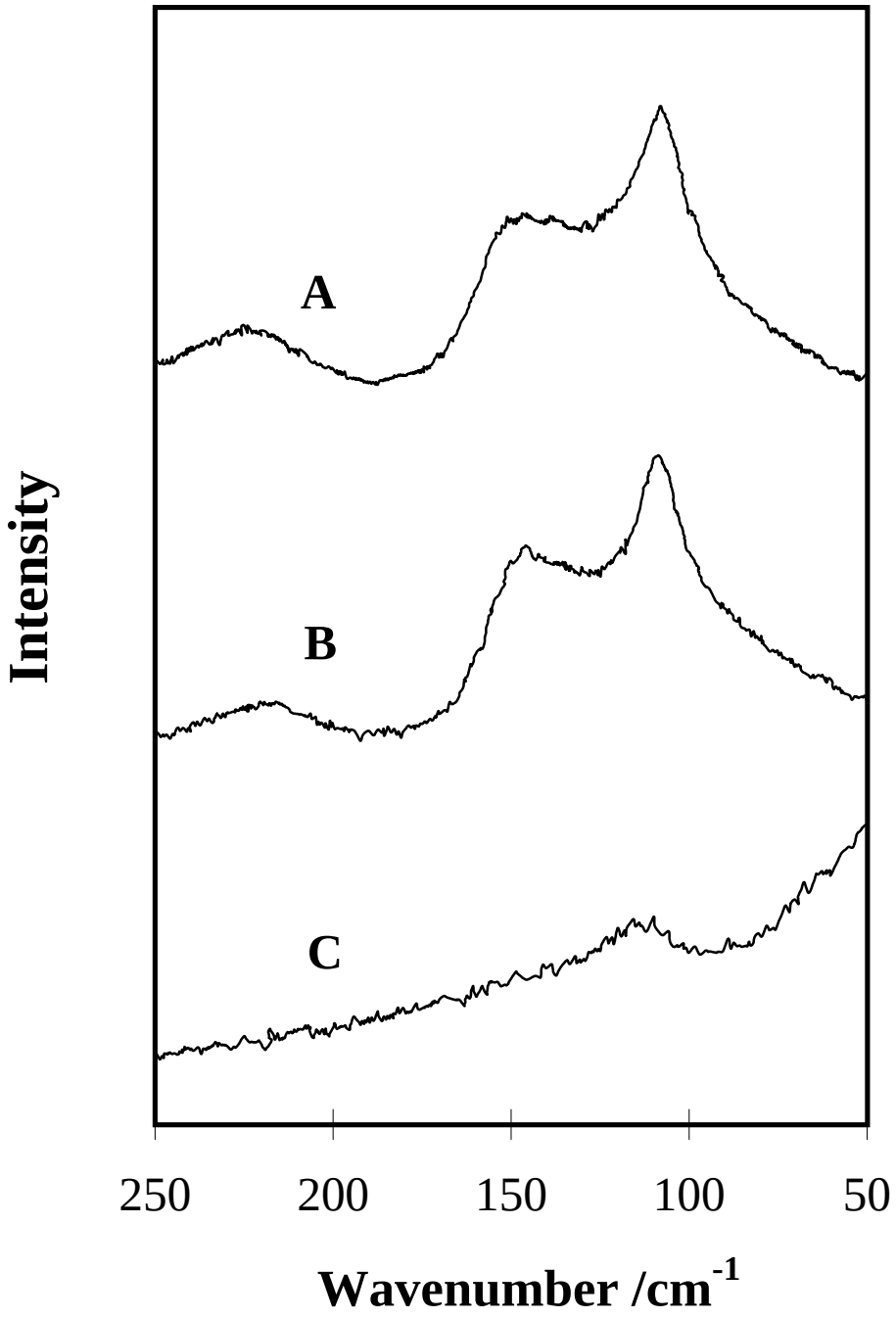

Fig.3 H. Yajima

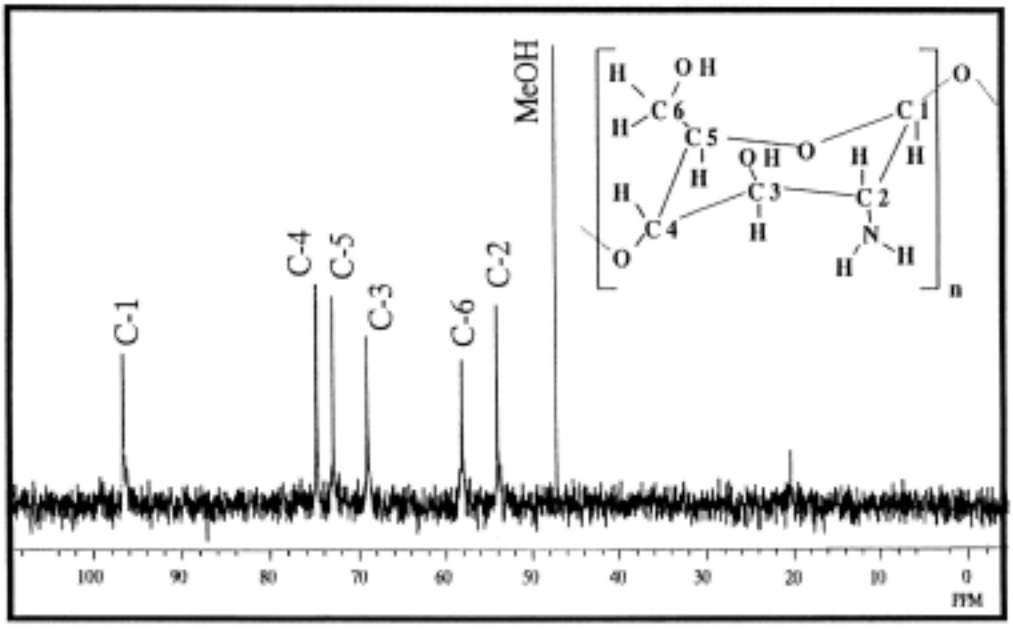

Fig. 4 H. Yajima

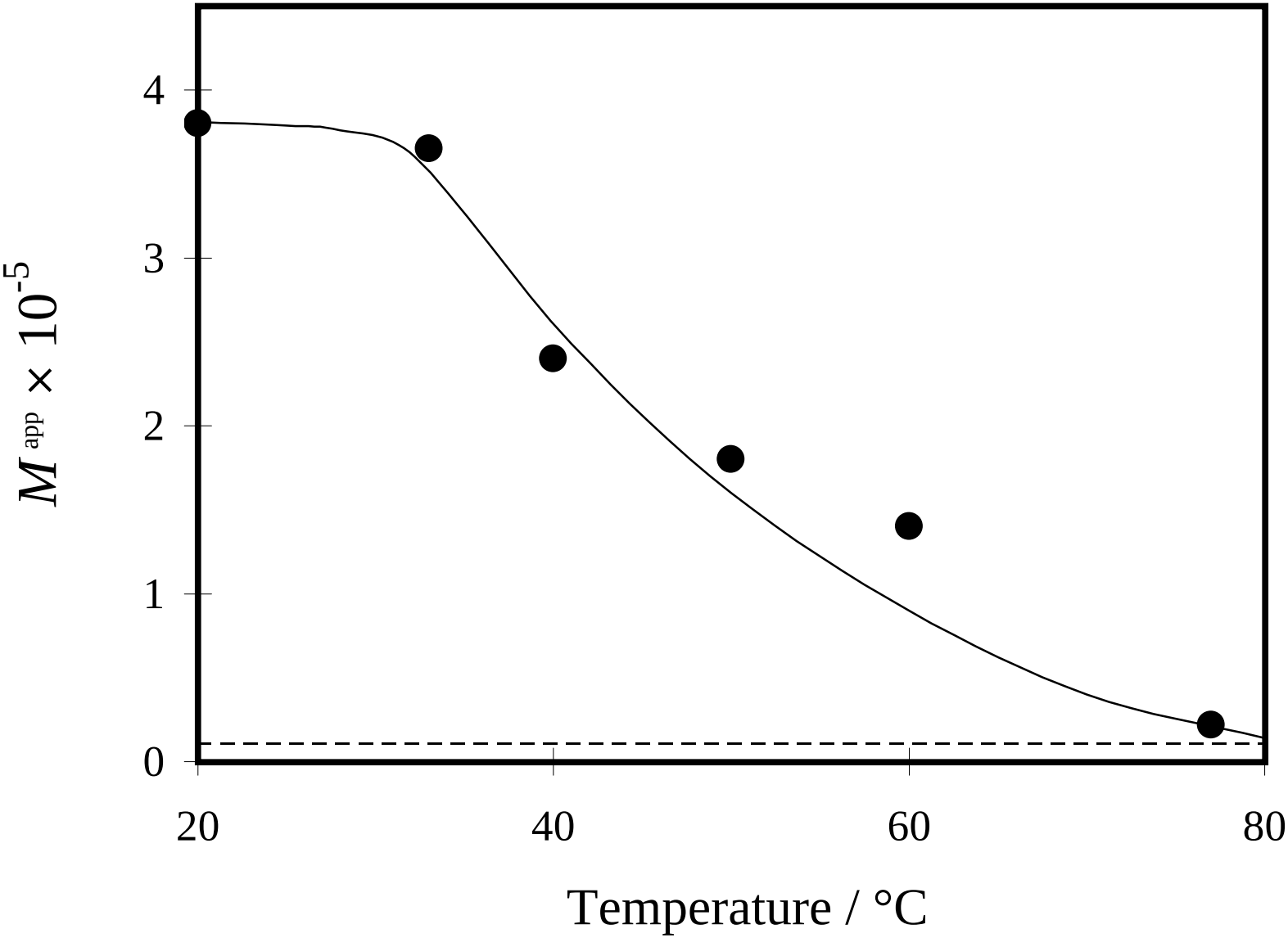

Fig.5 H.Yajima

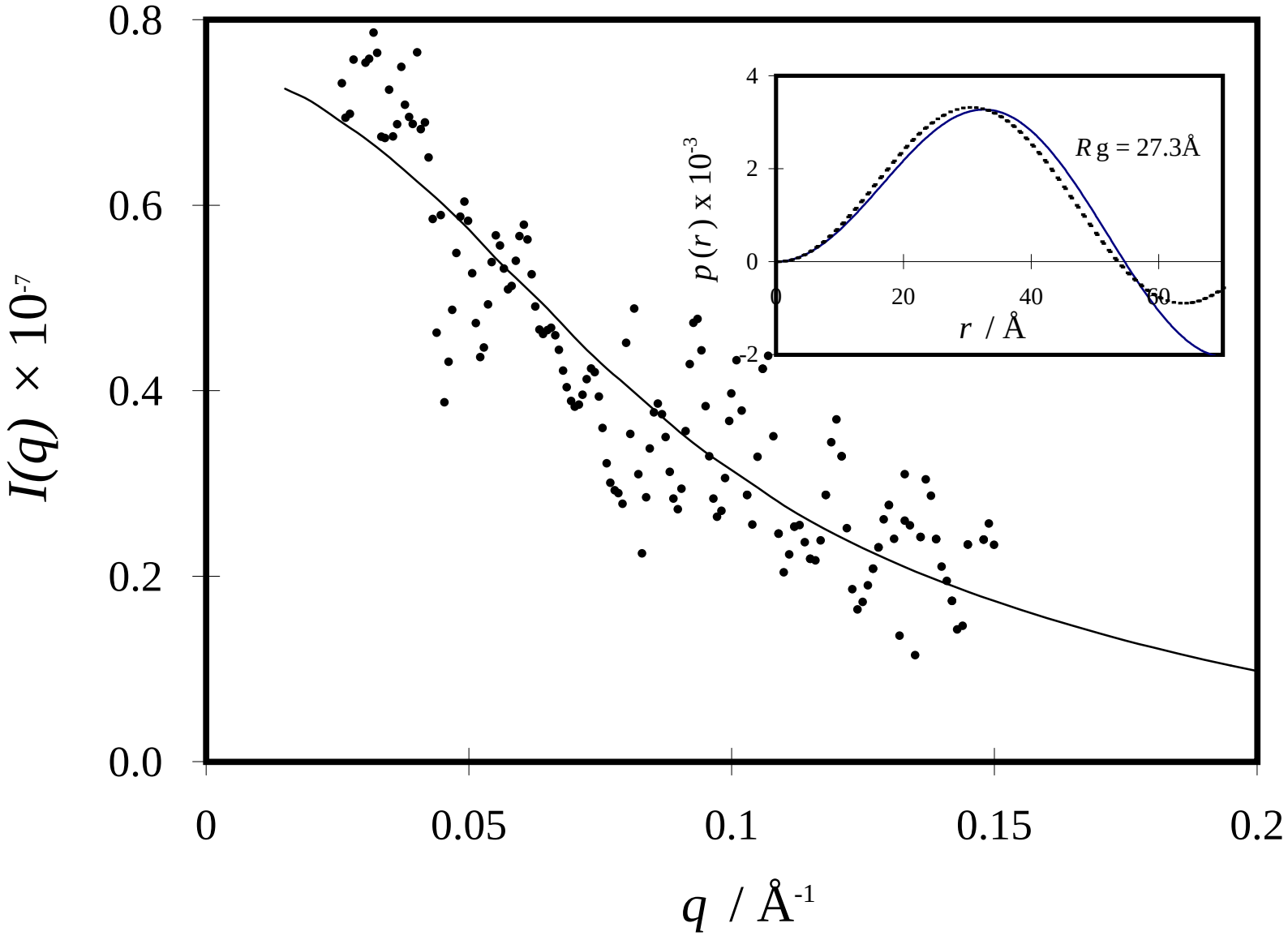

Fig.6(a) H. Yajima

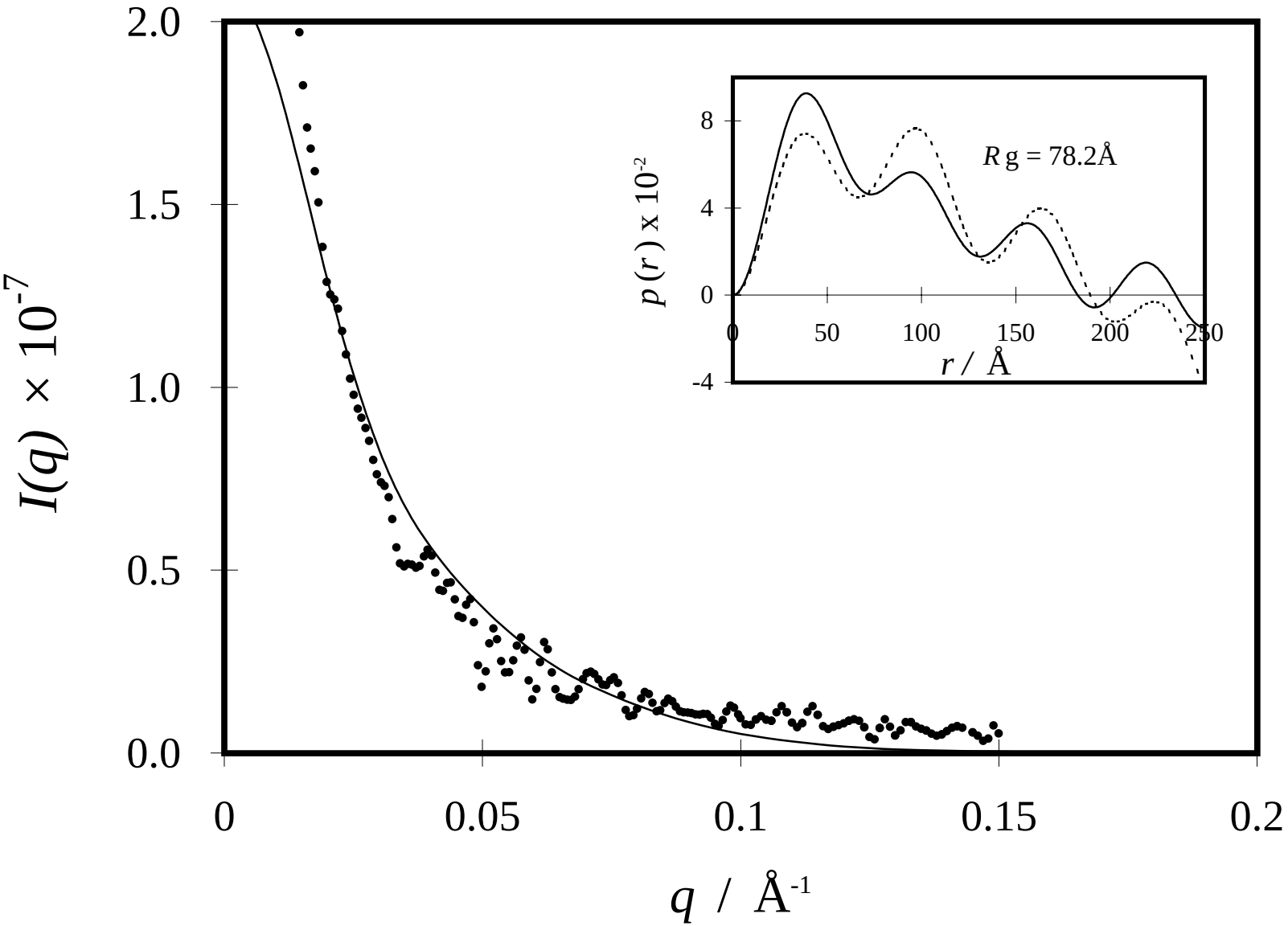

Fig.6(b) H. Yajima

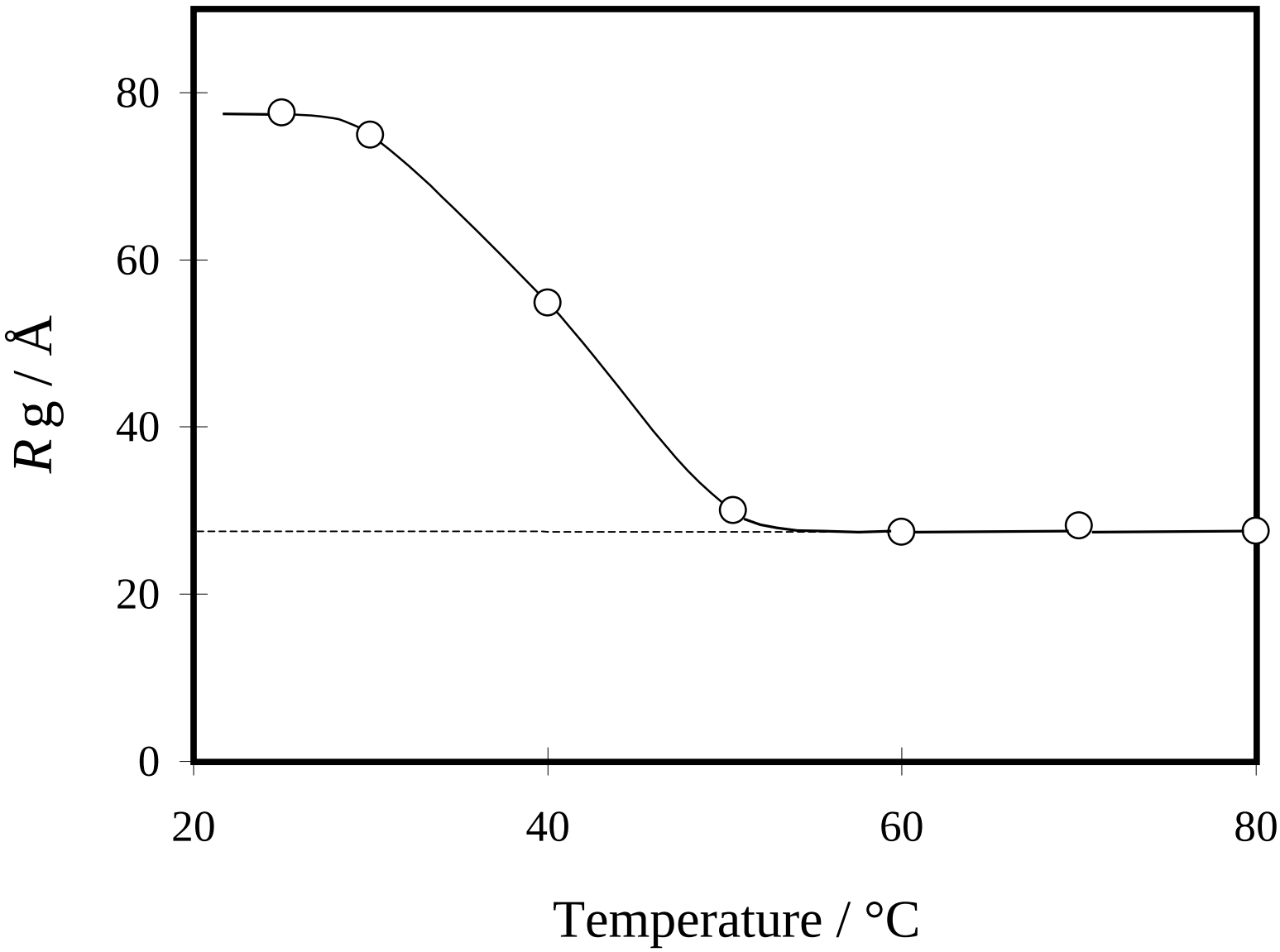

Fig.7 H. Yajima